Exchange interactions in NiO and at the NiO(100) surface

D. Ködderitzsch and W. Hergert

Fachbereich Physik, Martin-Luther-Universität Halle-Wittenberg, Friedemann-Bach-Platz 6, D-06099 Halle, Germany

W. M. Temmerman and Z. Szotek

Daresbury Laboratory, Daresbury, Warrington WA4 4AD, United Kingdom

A. Ernst

Max-Planck-Institut für Mikrostrukturphysik, Weinberg 2, D-06120 Halle, Germany

H. Winter

INFP, Forschungszentrum Karlsruhe GmbH, Postfach 3640, D-76021 Karlsruhe, Germany

The electronic and magnetic structure of bulk NiO and the NiO(100) surface is calculated using density-functional theory (DFT) in the local-spin-density (LSD) approximation including self-interaction corrections. We calculate the exchange coupling constants in bulk NiO and at the NiO(100) surface and show that in the case of bulk they agree better with experiment than the standard DFT calculations in the LSD approximation. We develop a model for the exchange interactions at the NiO(100) surface and discuss how they change from the surface to bulk.

I. INTRODUCTION

The $3d$ transition-metal monoxides (TMO's) and their surfaces exhibit a rich variety of electronic and magnetic phenomena, and they have attracted a lot of attention over the last decades, in particular concerning the nature of the band gap and the excitation spectrum in general.[1,2] After extensive experimental and theoretical studies of the bulk material the surfaces of the TMO's recently received a lot of interest. Fast progress in experimental techniques, such as x-ray magnetic linear dichroism[3] spectroscopy or x-ray-absorption spectroscopy[4] have proven valuable for studying the surface electronic and magnetic structure of TMO's. Glancing incidence X-ray diffraction has been used to detect an octopolar reconstruction at an electrostatically polar NiO(111) surface.[5] During the last decade or so transition-metal monoxides like MnO, NiO, CoO, and FeO have become more and more interesting for modern magnetoelectronics applications. Surface and interface effects such as spin disorder are of relevance to thin-film magnetoelectronics devices like spin valves, spin transistors, or spin-dependent tunneling devices. Recently, TMO's interfaces with ferromagnets have also attracted much attention due to their importance in advanced magnetoresistive devices.[6–8] Therefore, understanding the magnetic surface properties of TMO's and their interfaces with magnetic materials is crucial for potential technical applications.

In the ground state the above-mentioned TMO's crystallize in the rocksalt (NaCl) structure and exhibit antiferromagnetic magnetic ordering of type 2 (AF2), with planes of opposite spins being repeated in alternating order along the [111] direction defining two sublattices consisting of spin-up and spin-down metal ions, respectively. Below their respective Néel temperatures the magnetic ordering in TMO's is accompanied by a slight orthorhombic distortion. In the case of NiO the insulating state is characterized by a gap with a size of about 4 eV (Ref. 9) and a magnetic moment of about $1.7\mu_B$ (see references in Ref. 10). There are strong indications that NiO is a charge-transfer insulator—the top of the valence band is primarily formed by oxygen $2p$ states, while the bottom of the conduction band is Ni d-like.[9]

Due to the highly correlated nature of electron interaction in the TMO's, theoretical investigations employing *ab initio* methods to describe the electronic structure of these materials are difficult. Among them the standard density functional theory (DFT) in the local-spin-density (LSD) approximation has been proven to be inadequate for the calculation of certain properties of such oxides, predicting too small magnetic moments and gaps or even metallic behavior for CoO and FeO. In the case of NiO early LSD calculations gave a poor description of the ground state with the gap of about 0.2 eV and a magnetic moment of about $1\mu_B$,[11,12] in disagreement with experiment. Since in those calculations the top of the valence band and the bottom of the conduction band were predominantly Ni d-like, the gap was characterized as being of Mott-Hubbard type. Therefore, a series of approaches have been developed during the last decades to go beyond the DFT-LSD approximation. These methods include the LSD+U scheme[13] which gives the lower and upper Hubbard bands with the energy separation equal to the on-site Coulomb parameter U, the ``Hubbard I'' scheme for the local density approximation (LDA++) approach[14] for systems with strongly localized electrons, the self-interaction-corrected (SIC)-LSD method, which removes the unphysical self-interaction inherent in the LSD,[10,15] and the GW approximation, which takes into account a frequency- and orbital-dependent screening of the Coulomb interaction.[16] The most promising method however computationally demanding, appears to be the LSD+DMFT method combining band structure and many-body theory, the dynamical mean

field theory (DMFT).[17] Also, quantum chemical approaches, based on the Hartree-Fock method have been applied to TMO's.[18–21]

One of the main interests of experimental and theoretical studies of the antiferromagnetic oxides is the exchange coupling. To characterize the magnetic order two kinds of interactions are of relevance here: a direct nearest-neighbor (nn) exchange and an indirect next-nearest-neighbor (nnn) exchange of the superexchange type. Experimental information on the exchange coupling constants J_1 (nn interaction) and J_2 (nnn interaction) can be obtained from neutron scattering data[22] or magnetic susceptibility measurements.[23] To extract the values of J_1 and J_2 from the experimental data, the random-phase-approximation Green's function theory was utilized.[24–26] The relative signs and strengths of J_1 and J_2 reflect which type of magnetic order is realized in a bulk system where magnetic ions occupy positions on the fcc (face-centered-cubic) lattice, as this is the case for the TMO. For example, a strong antiferromagnetic nnn coupling and a weak ferromagnetic nn coupling is compatible with the AF2 magnetic ground state. Other magnetic ground states depending on the ratio of J_1 and J_2 are the antiferromagnetic state of type AF1, with planes of opposite spins being repeated in alternating order along the [100] direction, and the ferromagnetic (FM) state.[23]

The knowledge of the exchange integrals in the vicinity of a surface allows one to address issues of the surface critical behavior in the framework of mean-field theories. For Ising-like systems the surface exchange coupling J_S determines the kind of transition the surface undergoes while decreasing temperature. For J^S smaller than a critical value J_c^S the surface order is enforced by the bulk at the bulk critical temperature T_c^b, and this transition is labeled ordinary.[27] A special transition occurs for $J^S = J_c^{S}$[28] when both surface and bulk order independently at T_b^c. For $J^S > J_c^S$ an extraordinary transition[27] is obtained in which the surface orders when the bulk is still in the paramagnetic phase. By means of metastable helium atom diffraction Marynowski *et al.*[19] measured, for NiO, a surface Néel T_N temperature of 529 K, which is higher than the bulk T_N of 523.6 K and which they associated with an extraordinary antiferromagnetic transition on the NiO(100) surface.

For a consistent understanding of the exchange coupling phenomena it is crucial to perform *ab initio* calculations. Two different approaches are possible to extract the exchange constants from *ab initio* calculations; either to calculate the exchange constants directly,[29,30] or by means of mapping the total energies calculated for a series of different spin structures on a Heisenberg Hamiltonian.

In this paper we study a prototype TMO surface, namely, the (100) surface of NiO, using the SIC-LSD approach. In particular, we will determine and discuss differences between the electronic and magnetic properties in the bulk and at the surface. Owing to this we will be able to calculate not only the exchange coupling constants within the surface layer but also study the variation of J, layer by layer, starting from the surface inward. So far, the calculations based on embedded

cluster methods[20,21] have only been able to relate the bulk and the surface layer in-plane exchange coupling.

The remainder of the paper is organized as follows: in Sec. II we describe the SIC-LSD approach and its implementation. In Sec. III we present our results for the electronic and magnetic structures of bulk NiO to establish a benchmark comparison for the NiO(100) surface. The electronic structure of the NiO(100) surface and the corresponding exchange coupling constants are discussed in Sec. IV. A discussion of the present results in Sec. V concludes the paper.

II. SIC-LSD METHOD AND COMPUTATIONAL DETAILS

In the SIC-LSD formalism one defines a self-interaction free total energy-functional E^{SIC} by subtracting, from the LSD total energy functional E^{LSD}, the self-interaction of each occupied electron state ψ_α,[31] namely,

$$E^{SIC} = E^{LSD} - \sum_\alpha^{occ.} \delta_\alpha^{SIC}. \tag{1}$$

Here α numbers the occupied states, and the self-interaction correction for the state α is

$$\delta_\alpha^{SIC} = U[n_\alpha] + E_{xc}^{LSD}[\bar{n}_\alpha], \tag{2}$$

with $U[n_\alpha]$ being the Hartree energy and $E_{xc}^{LSD}[\bar{n}_\alpha]$ the LSD exchange-correlation energy for the corresponding charge density n_α and spin density $\bar{n}_\alpha = (n_\alpha^\uparrow, n_\alpha^\downarrow)$. Note that it is the LSD approximation which is the source of the spurious self-interaction, since the exact exchange-correlation energy E_{xc} has the property that, for any single-electron spin density $\bar{n}_\alpha$, it cancels exactly the Hartree energy

$$U[n_\alpha] + E_{xc}[\bar{n}_\alpha] = 0. \tag{3}$$

For truly extended states in the periodic solids the self-interaction vanishes. Consequently, the SIC-LSD approach can be viewed as a genuine extension of the LSD in the sense that the self-interaction correction is only finite for spatially localized states, while for Bloch like single-particle states E^{SIC} is equal to E^{LSD}. Thus the LSD minimum is also a local minimum of E^{SIC}. Now a question arises of whether there exist other competitive minima, corresponding to a finite number of localized states, which could benefit from the self-interaction term without losing too much band formation energy. This usually will be the case for rather well localized electrons like the $3d$ electrons in transition-metal oxides or the $4f$ electrons in rare-earth compounds. It follows from Eq. (1) that within the SIC-LSD picture such localized electrons move in a different potential than the normal delocalized valence electrons which respond to the effective LSD potential. For example, in the case of NiO, eight Ni d electrons move in the SIC potential, while all the other electrons "feel" only the effective LSD potential. Thus, by including an explicit energy contribution for an electron to localize, the *ab initio* SIC-LSD approach describes both localized and delocalized electrons on an equal footing, leading to a greatly improved description of static Coulomb correlation effects over the LSD approximation. Assuming various

atomic configurations, consisting of different numbers of localized states, one can explore the corresponding local minima of the SIC-LSD energy functional of Eq. (1), and determine the lowest-energy solution. The hope is that for such systems as transition-metal oxides or rare-earth compounds the lowest energy solution will describe the situation where some single-electron states may not be of Bloch-like form.

In the present work the SIC-LSD approach has been implemented[15,32,33] using the linear muffin-tin-orbital (LMTO) band-structure method[34] in the tight-binding representation,[35] where the electron wave functions are expanded in terms of the screened muffin-tin orbitals, and the minimization of E^{SIC} becomes a nonlinear problem in the expansion coefficients. The atomic spheres approximation (ASA) has been used, according to which the polyhedral Wigner-Seitz cell is approximated by slightly overlapping atom centered spheres, with a total volume equal to the actual crystal volume.

Since the NaCl structure of NiO is an open one, we have explored two different setups for the calculations—one in which the ASA spheres have been associated only with the sites of the sodium chloride structure, and another in which in addition a number of empty spheres (ES's) have been introduced on interstitial sites. In the first case the ASA radii have been chosen to be 2.70 and 2.16 a.u. for Ni and O, respectively, and in the second case we have used ASA spheres of 2.52, 2.10, and 1.41 a.u., for Ni, O, and the ES, respectively. Inside each sphere the potential has been assumed spherically symmetric. One energy panel has been considered when constructing the LMTO's. With respect to the basis functions, on all the Ni sites the s, p, and d partial waves have been treated as low waves; for oxygen the s and p states have been described as low waves, with d states being downfolded[36]; and for ES's s low waves and downfolded p waves have been considered. The surface has been modeled by a periodic repetition of NiO slabs separated by vacuum which is represented here by layers of ES's with s partial waves treated as low waves, and p waves being downfolded. A setup consisting of seven layers of NiO and five layers of ES's has been found to be adequate for eliminating the interaction of the opposed NiO(100) surfaces and reproducing δ bulk like electronic structure in the middle of the NiO slab. In the vacuum layers the nickel and oxygen ASA spheres have been replaced by two types of ES's with their respective radii kept to preserve the NaCl structure of the slab.

In order to discuss the relation between the bulk and the change of its electronic and magnetic structure when introducing a termination by a surface we have first investigated the bulk. Also, this way we have been able to define the most realistic basis set of parameters (choice of basis set, ASA-sphere radii, etc.) which describes the bulk electronic structure adequately and makes the surface calculations feasible at the same time. In all calculations the lattice constant of NiO has been assumed to be 4.193 Å (7.924 a.u.).[37] The experimentally observed orthorhombic distortion of the lattice has been neglected in this work

TABLE I. Comparison of different magnetic structures of bulk NiO within the SIC-LSD method. $\Delta N_{Ni} = N_{Ni}(E_F) - N_{Ni}^{AF2}(E_F)$ is the difference beween the charge in the Ni-ASA-sphere for a given magnetic ordering relative to the AF2 ordering. In the ground state (AF2) the experimental gap and magnetic moment are reported to be about 4.3 eV[9] and $\approx 1.7 \mu_B$ (see Refs. in Ref. 10), respectively.

	Gap in eV	ΔN_{Ni} in e	$|\mu|/\mu_B$ on Ni	$|\mu|/\mu_B$ on O	$(E - E^{AF2})$ in meV/formula unit
AF2	2.78	0.000	1.56	0.00	0.00
AF1	1.36	0.016	1.69	0.12	152.93
FM	1.56	0.009	1.66	0.34	115.95
AF2 ES	3.02	0.000	1.58	0.00	0.00
AF1 ES	1.52	0.019	1.70	0.12	135.20
FM ES	1.75	0.013	1.67	0.33	106.41
AF2, LSD	0.25		1.03	0.00	

III. RESULTS FOR BULK NiO

A. Electronic and magnetic structure

In order to find the absolute minimum of the SIC-energy functional [Eq. (1)], one has to explore various manifolds of localized and delocalized states. For bulk NiO it turns out that self-interaction correcting only the eight Ni d states leads to the absolute minimum of Eq. (1).[15] In cubic NiO the spin-up and -down d states are separated by the exchange splitting, and the crystal field then splits the d bands into t_{2g} and e_g subbands (the antiferromagnetic ordering lowers the symmetry further, but one can still identify states as t_{2g} or e_g). In the bulk, the SIC-LSD total energy is minimized by applying SIC to five majority Ni d electrons and three minority t_{2g} electrons for all the magnetic structures. Apart from the AF2 magnetic structure of NiO, in the present work we have also studied the AF1 structure and the FM structure. In order to consistently compare the different structures and to suppress errors due to different Brillouin-zone summations all the calculations have been carried out using the same unit cell containing eight formula units. This is important as one expects the energy differences due to changes in the magnetic ordering to be very small. The results of the SIC-LSD calculations for energy gaps, magnetic moments, and total energy differences are given in Table I. Note that the size of the gap varies with the magnetic ordering, and the largest gap is obtained for the AF2 magnetic phase. One should mention here that its size is slightly sensitive to the choice of the basis functions and the sphere radii. For example, with f waves included on the Ni sites in the setup with ES's, one can obtain a gap of 3.45 eV. However, since the size of the eigenvalue problem increases substantially when studying surfaces, in this paper we have restricted ourselves to a minimum but adequate basis set. With respect to the character of the gap, it can be seen in Fig. 1, showing the NiO density of states (DOS) for three magnetic orderings, that in our calculations NiO appears to be a charge-transfer insulator and this is independent of the magnetic order. The top of the valence band is predominantly oxygen $2p$-like, with a small admixture of Ni-d states, whereas the bottom of the conduction band has Ni-d character in all the magnetic
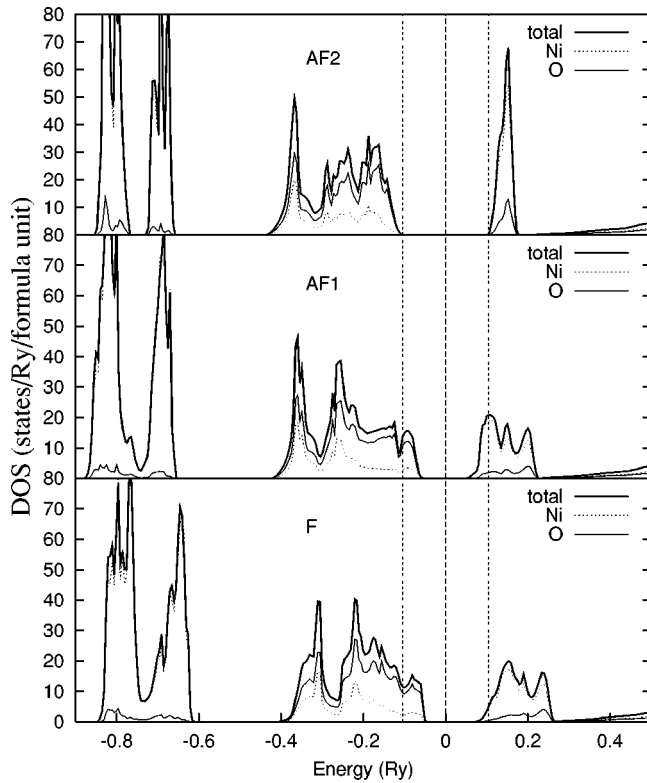
FIG. 1. Density of states for different magnetic orderings of NiO as calculated by the SIC-LSD method. Energies are quoted with respect to E_F. The vertical dashed line at energy zero marks E_F, and the dotted lines refer to the gap edges in the AF2 ordering.

FIG. 2. Spin resolved Ni-d DOS for different magnetic orderings of NiO as calculated by the SIC-LSD method and decomposed into t_{2g} and e_g contributions. Energies are quoted with respect to E_F. The vertical dashed line refers to E_F.

structures considered. In the AF1 and FM structures a broadening of the Ni-d conduction band is observed. Furthermore for these two magnetic orderings the lower Ni-d bands do not exchange split anymore as compared to AF2.

The variation of the gap and the broadening of bands in the AF1 and FM magnetic phases, as compared to the AF2 magnetic structure, can be readily explained by analyzing the formation of bands (also see Terakura *et al.*,[11]). Important here is the observation that the TMO's exhibit a strong coupling of the second-nearest-neighbor cations via oxygen p orbitals. This coupling is of $dd\sigma$ type connecting e_g orbitals. Two consequences will then determine the size of the gap depending on the magnetic ordering. First, in the AF2 magnetic ordering e_g orbitals of *oppositely* polarized Ni ions are coupled via an oxygen bridge, whereas in the AF1 and FM phases the *like* polarized ions are coupled that way. As spin-conserving hopping between nnn's is suppressed in the first case; so is the broadening of bands leading to a larger separation of the subband edges. Second, the intersublattice coupling in AF2 causes a pronounced splitting of e_g states between minority- and majority-spin bands in contrast to AF1 or FM ordering (compare also to Fig. 2).

In the LSD-only calculation for NiO, we have not been able to stabilize either the AF1 or FM solution. This was also observed by Terakura *et al.*,[11] who concluded that for NiO the LSD could stabilize the gap in the AF2 ordering only (using the above sketched *gedankenexperiment* for the formation of bands). In MnO, on the other hand, one can obtain
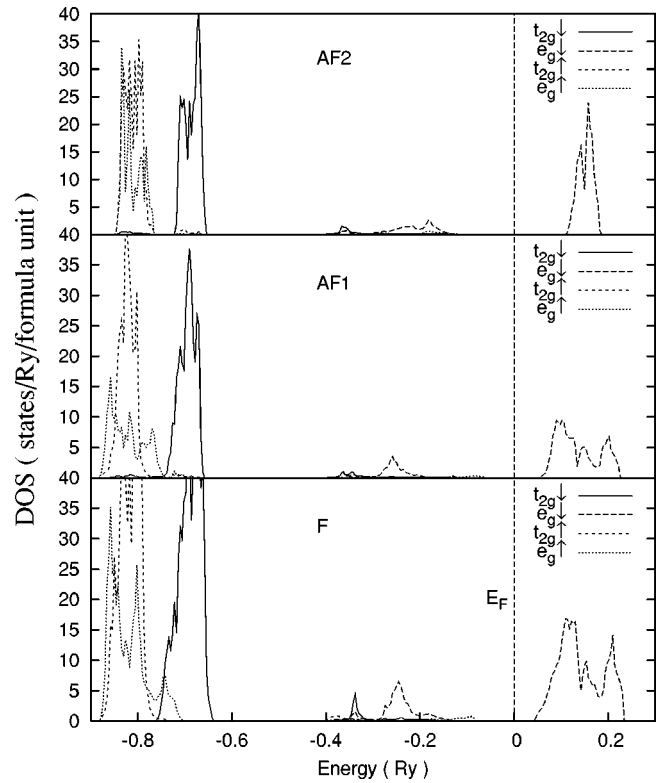
magnetic solutions for all three magnetic structures, but the insulating character has only been observed for the AF2 ordering. Note, however, that the LSD completely failed to provide the insulating state for CoO or FeO. Improvements, using the generalized gradient approximation (GGA) to the local density approximation (LDA),[38] yielded a small indirect gap for CoO but still gave a metallic behavior for FeO. It seems worth mentioning here that an insulating paramagnetic state for TMO's cannot be realized within the LDA, LDA+U, or SIC schemes. However, e.g., the "Hubbard I" scheme of the LDA++, which takes into account dynamic effects in order to overcome the shortcomings of the mean-field approximation inherent in those other schemes, gives, for NiO, a pseudogap of roughly 3.5 eV in the paramagnetic state.[14]

The SIC-LSD magnetic moment on Ni varies only slightly in the different orderings. In the case of the AF2 structure the oxygen has no magnetic moment, whereas in the AF1 it has a small moment of $0.12\mu_B$. In the FM ordering oxygen develops a moment such that the whole moment per formula unit is $2.0\mu_B$. This follows from the fact that in this case the occupied bands are completely filled and separated from the unoccupied bands by a gap resulting in an integer magnetic moment per formula unit (measured in μ_B).

As can be seen from the last column of Table I, the SIC-LSD predicts the AF2 solution as the ground state magnetic ordering followed by FM and AF1 solutions. The ratio of the energy differences between FM-AF1 and FM-AF2 solutions

TABLE II. Exchange constants (in meV) for bulk NiO.

	SIC-LSD	SIC-LSD(ES)	LSD (Ref. 41)	Exp. (Ref. 22)
J_1^b	2.3	1.8	5.3	1.4
J_2^b	-12	-11	-106	-19

is about 3. The same order of total energies and similar ratio were also obtained by a Hartree-Fock calculation,[18] although the absolute values of the energy differences were smaller.

There are small but noticeable charge redistributions between the ASA spheres of Ni and O when comparing the different magnetic orderings. Interestingly, the ES's included in the second setup of the calculations carry the same amount of charge, irrespective of the magnetic order, indicating that the redistribution of charge is occurring at the Ni-O bridge. In summary, the SIC-LSD gives reasonable gaps and magnetic moments, correctly predicts AF2 as the ground state, and describes NiO as a charge transfer insulator.

B. Exchange coupling constants

To facilitate a quantitative analysis of the magnetic properties of NiO, as well as to establish a benchmark for the surface calculations, in this subsection we present calculations for the bulk exchange coupling constants. To model the exchange interactions in this compound we use the Heisenberg spin Hamiltonian

$$H = -\sum_{ij} J_{ij} \mathbf{S}_i \cdot \mathbf{S}_j, \tag{4}$$

with $J_{ii} = 0$. We rewrite this equation as

$$H = -\sum_{ij} J_{ij} S^2 \sigma_i \sigma_j, \tag{5}$$

with S being the total spin of the ion (here $S = 1$) and $\sigma_i \in \{-1, 1\}$ having only two values (any canting of moments is neglected). Here we include only J's which couple nearest (J_1) and next nearest (J_2) neighbor sites. As mentioned above, NiO reveals a small distortion from the cubic structure, caused by exchange striction effects, resulting in somewhat different exchange constants $J_1^\pm$ below the Neél temperature.[39,40] In this work, however, we neglect this effect and consider the ideal rocksalt structure only.

Using Eq. (4) the respective bulk coupling constants J_1^b and J_2^b can be expressed via total-energy differences per formula unit of the different magnetic orders as

$$J_1^b = \frac{1}{16}(E^{AF1} - E^F),$$

$$J_2^b = \frac{1}{48}(4E^{AF2} - 3E^{AF1} - E^F). \tag{6}$$

The resulting J_1^b and J_2^b, for both setups, excluding and including ES's, together with the standard LSD calculations and the experimental values, are given in Table II. Note that the SIC-LSD results for both setups are fairly similar. Com-
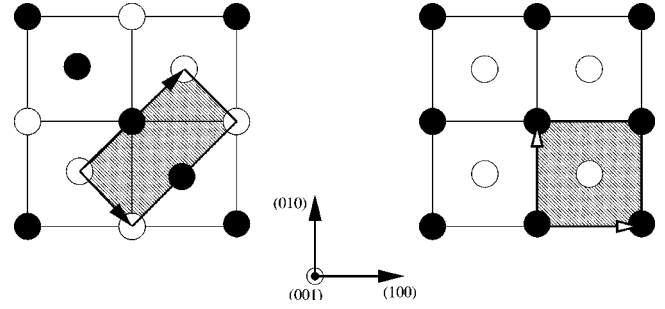

FIG. 3. Surface unit cells for the slabs. Black and white circles represent Ni up and down, respectively. Oxygen has been omitted. The left we denote as AF2 geometry, the right as AF1 geometry.

paring the SIC-LSD values to experiment and the LSD calculations one can see that SIC-LSD approach remedies most of the errors of the LSD, however leading to smaller values for J_2^b than those given by experiment. The huge overestimate of the exchange constants by the standard LSD can be attributed to its failure in describing the localized nature of the Ni d electrons. On the other hand, the SIC-LSD approach overestimates this localization, leading to somewhat too small values for the nnn coupling.

It is interesting to mention that the unit cell used in these calculations allows one to realize other magnetic orderings than AF1, AF2, and FM, utilized here for determining $J_{1,2}^b$. Of course, using the other possible magnetic orderings one arrives at sets of equations for the exchange coupling constants different from Eq. (6). However, reassuringly, we have found that all sets of equations have given nearly the same values for the coupling constants, thus indicating that our total energies are reliable and the inclusion of only nn and nnn terms is sufficient for describing the magnetic interactions.

IV. RESULTS FOR NiO(100)

Low-energy electron diffraction data give the (100) surface of NiO to be a termination of the bulk-crystal structure showing no reconstruction and small inward relaxations of surface layers which is, however, very small (less than 2%).[42,43] Early low-energy electron-diffraction studies of the surface spin ordering on the NiO(100) surface report a 2 ×1 surface magnetic structure[44] suggesting a bulk termination. More recent experiments employing metastable two ^{3}S helium atom diffraction[19] confirm the 2×1 antiferromagnetic ordering at the surface, originating from a termination of the AF2 bulk magnetic structure. Therefore, in our theoretical study, we have first explored the electronic structure of a surface exhibiting this particular magnetic order, namely, the (100) surface.

A. Electronic structure of the (100)-surface

To study the (100) surface, obtained by an ideal termination of the AF2 ordered bulk, we have used a surface unit cell consisting of two formula units of NiO per layer as shown in Fig. 3. Although in the case of bulk the inclusion of ES's at the interstitial sites of the NaCl structure has been of
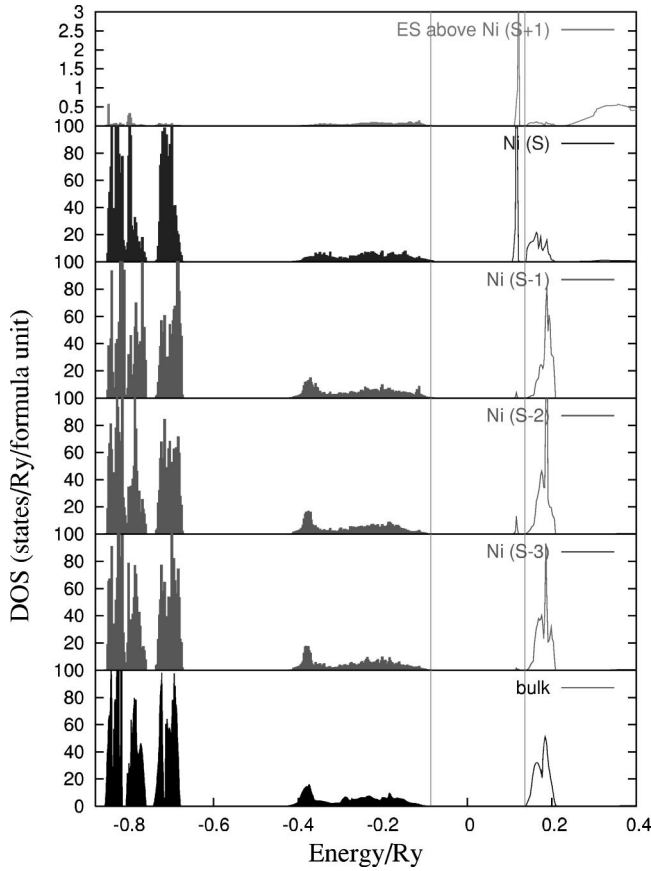
FIG. 4. Layer-resolved SIC-LSD DOS projected onto Ni-3*d* states. The top panel shows the DOS projected onto the ES above the top Ni ion in the first vacuum layer. Vertical lines at the opposite edges of the gap are meant to help in visualizing the decrease of the gap as compared to the bulk (bottom panel).
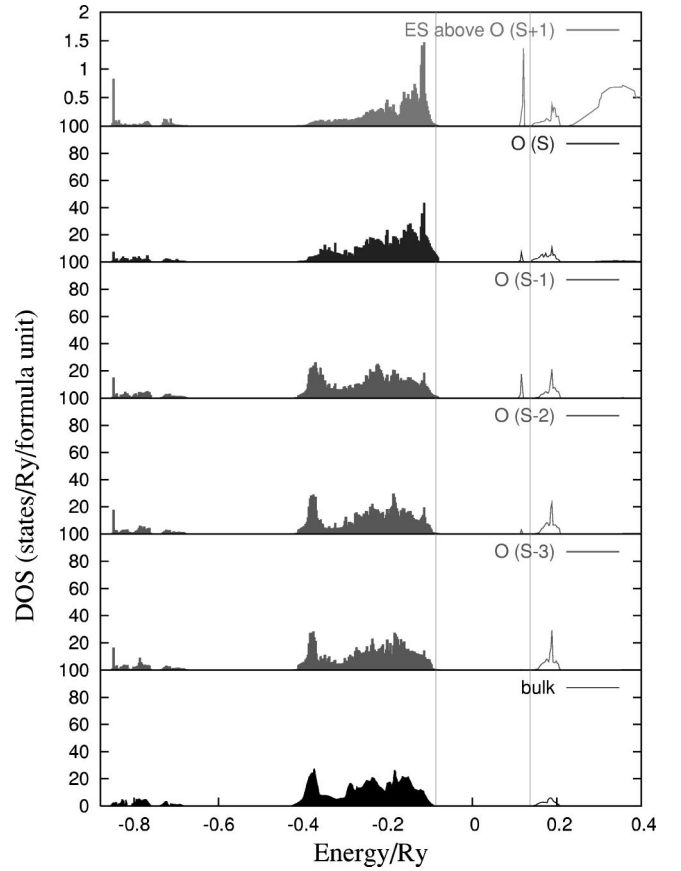
FIG. 5. SIC-LSD DOS projected onto O-2*p* states. The top panel shows the DOS projected onto the ES above the top O ion in the first vacuum layer.

secondary importance, in the case of the surface they have been crucial for obtaining meaningful results for its electronic and magnetic properties. The ASA radii have been chosen as in the bulk calculations.

In Figs. 4 and 5, the layer resolved SIC-LSD DOS, associated with the nickel and oxygen spheres, are shown. Additionally, the DOS of ES in the first vacuum layer is displayed. First of all one notices that the innermost layer ($S-3$) of the slab has a very much bulklike DOS—the perturbation introduced by the surface diminishes very fast which is also reflected through a bulklike charge and spin moment on the ASA spheres in this layer. Furthermore, two sharp peaks at the opposite edges of the gap become apparent. As these states are confined to the vicinity of the surface layer (S) they are identified as surface states. These surface states give rise to the highest density of states in the ES above the nickel and oxygen spheres. A detailed analysis shows that the state at the bottom of the conduction band in the top layer is formed by nickel states which have predominantly a d_{z^2} character, whereas the states at the top of the valence band are oxygen p_z like. These surface states have also been found in an LDA+U study,[45] and they are due to an energy shift of the oxygen p_z-orbital and the nickel d_{z^2} orbital as compared to the oxygen p_x,p_y and the nickel $d_{x^2-y^2}$ orbitals,

respectively[46] (in the bulk the three oxygen p states and the two nickel e_g states are degenerate). The reason for the splitting of energy levels is the reduction from cubic symmetry to C_{4v} at the surface. From Figs. 4 and 5 it is also apparent that the gap which separates the occupied and unoccupied states decreases in the vicinity of the surface. This can be attributed to the Madelung potential shift caused by the missing half-space of the crystal as compared to the bulk, and has already been pointed out by Pothuizen *et al.*[21]

B. Magnetic interactions at the surface

Having in mind the geometry (Fig. 6) of the problem we can write the total energy of the mth magnetic configuration of the supercell as

$$E^{(m)} = \sum_i^{sites} E^i - \sum_{ij}^{\parallel} J_\parallel^{ij} S^2 \sigma_i \sigma_j - \sum_{ij}^{\perp} J_\perp^{ij} S^2 \sigma_i \sigma_j. \quad (7)$$

Here the total energy has been split up into three contributions: (a) a term comprising all on-site energies E^i, (b) a term describing the coupling within the layers ($J_\parallel^{ij}$), and (c) a term composed of energy contributions from coupling between the layers ($J_\perp^{ij}$).

To extract the coupling constants one has to find a suitable set of magnetic configurations which yield the exchange con-
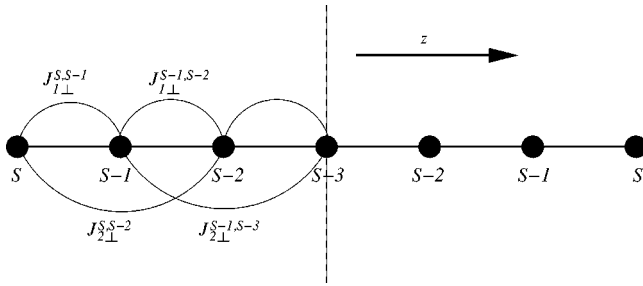
FIG. 6. Slab geometry. Determining the perpendicular exchange coupling constants $J_{1,2\perp}$ simplifies the modeling to a linear chain with weights attached to the coupling constants connecting the layers.

stants by mapping the calculated SIC-LSD total energies onto the Heisenberg Hamiltonian. Given a magnetic configuration and flipping a spin on a particular site will affect all terms coupling to this site. In other words, if one keeps the magnetic order within the layers the same and changes only the ordering, layer by layer, one can collect information required for determining the perpendicular coupling constants $J_\perp^{ij}$ in Eq. (7). Following this idea it turns out that the terms in E^i and $J_\parallel^{ij}$ cancel as the J's are calculated from differences of total energies $E^{(m)}$. This way one can extract from all possible equations for magnetic structures those which contain only the exchange constants mediating the coupling between the layers ($J_\perp^{ij}$). This is very convenient as it allows for using setups having only one NiO formula unit per layer, thus reducing the calculation time for the different magnetic structures.

Concentrating on working out the values of the exchange coupling constants connecting the subsequent layers, we have considered only magnetic configurations that are symmetric with respect to the central plane (see Fig. 6) and in all of them the transition-metal ions are coupled ferromagnetically within the planes. For a seven-layer slab one therefore has eight possible magnetic configurations which are given in Table III, together with a matrix of coefficients. As there are only five exchange coupling constants to be determined, one has the freedom to choose different sets of equations to calculate the J's. This also gives a possibility to cross-check the results. For checking convergence with respect to the slab thickness we have in addition considered a slab with 11 layers of NiO, and we shall come back to that later.

Since the energies involved in the magnetic interactions are small as compared to the total energy of the whole supercell, one has to ensure convergence with respect to the number of **k** points and the number of atoms included in the cluster used for the evaluation of the tight-binding structure constants. It has turned out that the *energy differences*, used in the determination of the exchange-coupling constants, converge much more rapidly with respect to the number of **k** points than the *total energies* which has been beneficial for the overall calculations. Typically, we have used 25 **k** points in the surface Brillouin zone and two along the direction perpendicular to the surface.

In Table IV the calculated values of the exchange constants are given both for the seven- and eleven-layer slabs. The results show that the perpendicular exchange constants, coupling the surface layer (S) to lower-lying layers $J_{1\perp}^{S,S-1}$ and $J_{2\perp}^{S,S-2}$, are enhanced at the surface by 20–30% as compared to those in the middle of the slab and to the respective bulk values of 1.8 and -11 meV. All deeper-lying coupling constants are essentially unaffected and compare very well to the respective bulk values. This shows that the effect of cutting off a half-space of the crystal has only a local impact on the exchange coupling. From these findings one can infer that if the in-plane coupling constants are deviating from the bulk values, only those within the surface will be affected. This then limits the number of magnetic configurations to be taken into account. Note that having more equations at our disposal than needed for extracting the five perpendicular coupling constants corresponding to the seven-layer setup, we have been able to check the consistency of results with respect to different sets of equations. As can be seen in Table IV this consistency has been fulfilled. Using a slab consisting of 11 layers of NiO we could also extract exchange constants for deeper layers and ensure convergence with respect to the slab thickness of our supercell calculation.

For a determination of the in-plane exchange coupling constants $J_\parallel$, two formula units per layer are needed to allow for spin-flips within the plane. The simultaneous determination of the in-plane nn and nnn exchange interactions requires a surface unit cell consisting of at least four formula units of NiO which would have substantially increased the size of the eigenvalue problem. Instead, we have chosen to use two individual setups denoted as AF1 and AF2 geom-

TABLE III. Coefficients for the exchange coupling constants for a seven-layer slab of NiO for different magnetic configurations.

m	Spin conf. $E^{(m)}$	$J_{1\perp}^{S,S-1}$	$J_{1\perp}^{S-1,S-2}$	$J_{1\perp}^{S-2,S-3}$	$J_{2\perp}^{S,S-2}$	$J_{2\perp}^{S-1,S-3}$
1	+ + + + + + + +	-32	-32	-32	-8	-8
2	+ − + − + − + − +	32	32	32	-8	-8
3	− − + + + − −	-32	32	-32	8	8
4	− + + − + + −	32	-32	32	8	8
5	− + + + + + −	32	-32	-32	8	-8
6	− − − + − − −	-32	-32	32	-8	8
7	− + − − − + −	32	32	-32	-8	8
8	− − + − + − −	-32	32	32	8	-8

TABLE IV. Exchange coupling constants $J_{\perp 1,2}$ in meV for seven- and 11-layer slabs. Two values are quoted for the seven layer slab, referring to two different sets of equations (see the text) used for the determination of the coupling constants.

	7 layer (1)	7 layer (2)	11 layer
$J_{1\perp}^{S,S-1}$	2.10	2.08	2.08
$J_{1\perp}^{S-1,S-2}$	1.69	1.67	1.69
$J_{1\perp}^{S-2,S-3}$	1.67	1.66	1.71
$J_{1\perp}^{S-3,S-4}$			1.74
$J_{1\perp}^{S-4,S-5}$			1.66
$J_{2\perp}^{S,S-2}$	-15.60	-15.54	-14.71
$J_{2\perp}^{S-1,S-3}$	-11.23	-11.31	-11.31
$J_{2\perp}^{S-2,S-4}$			-11.57
$J_{2\perp}^{S-3,S-5}$			-11.74

etries to determine the in-plane exchange constants separately (see Fig. 3), allowing for spin-flips within the planes.

To determine $J_{1\parallel}^{S}$ we used the slab with the AF1 geometry. In addition to configurations $E^{(1)}$ and $E^{(5)}$ of Table III, we have calculated the total energy of a configuration which differs from $E^{(1)}$ by flipping one of the two Ni spins in the surface layer. In this configuration ($E^{(9)}$) the Ni ions are coupled antiferromagnetically (type 2) in S and ferromagnetically in all the other layers. Then $J_{1\parallel}^{S}$ is given by

$$J_{1\parallel}^{S} = \frac{1}{64}(2E^{(9)} - E^{(1)} - E^{(5)})$$

for the seven-layer slab.

To extract $J_{2\parallel}^{S}$ we have used three setups of AF2 geometry, one with an ideal AF2 magnetic ordering and two with keeping all but the surface layer in the ideal AF2 magnetic ordering. In the latter two configurations spins in S were flipped so that we obtained ferromagnetic coupling in S (E^{fm}) or antiferromagnetic coupling in S (E^{af}) while coupling ferromagnetically to ($S-2$)

$$J_{2\parallel}^{S} = \frac{1}{64}(E^{AF2} + E^{af} - 2E^{fm}) - \frac{1}{4}J_{1\parallel}^{S}.$$

With these formulas and the determined energies we have evaluated the in-plane exchange coupling constants to be $J_{1\parallel}^{S} = 1.66$ meV and $J_{2\parallel}^{S} = -9.52$ meV, respectively.

V. DISCUSSION

Let us discuss in more detail how the present results relate to earlier studies of the subject. Up to now different scenarios have been discussed in literature. Pothuizen *et al.*[21] argued, based on an ionic model, the Zaanen-Sawatzky-Allen model,[47] that the exchange constant at the surface should be enhanced by 50%. They were reasoning that the decrease of the Madelung potential at the surface, leading to a lowered charge-transfer energy Δ, should enlarge the surface exchange coupling by a factor of 1.5 for all the TMO's. Configuration-interaction (CI) calculations using a cluster

approach, where Ni_2O or a Ni_2O_9 clusters were embedded into a field of point charges,[48] predicted the opposite behavior, namely that the value of J_2 should be decreased by 20% as compared to the respective bulk value. Further analysis showed that the reduced coordination number of the Ni cations plays a key role in the decrease of the effective coupling constant, whereas the reduction of the Madelung potential is negligible as compared to that. Our results confirm this finding showing a slight decrease of $J_{2\parallel}^{S}$ as compared to the respective bulk value. Cluster CI calculations become very demanding when the size of the cluster becomes larger than those used in the calculation mentioned, which basically inhibits their extension to larger systems. On the other hand, our approach allowed us to consider the full environment of the surface cations, i.e., the coupling to deeper-lying layers.

Using the determined values of the in-plane ($J_{\parallel}$) and perpendicular ($J_{\perp}$) exchange constants in the Heisenberg Hamiltonian [Eq. (5)] one can show that for the (100) surface the ideal AF2 termination of the bulk is energetically favored, which is consistent with the experimental observation of a 2×1 magnetic surface cell. One can arrive at the same conclusion by simple consideration relating the magnitudes of the surface exchange coupling constants to the ground-state AF2 bulk values.

To shed some light on the stability of the ordering at the surface, let us compare the magnetic contribution to the total energy [via Eq. (5)] of atoms residing in the bulk and at the surface. The AF2 ground state would be destabilized by increasing the magnitude of the nn FM coupling, characterized by a positive J_1, and stabilized by increasing the magnitude of AF nnn coupling, characterized by a negative J_2. Therefore, the ratio of both these energy contributions represents a measure of the stability of this particular ordering in a given geometry at $T=0$. Focusing on a particular atom in the bulk on a fcc lattice, there are 12 nn couplings via J_1 and six nnn couplings via J_2 to it. The ratio of these energy contributions is then given by $6J_2^b/12J_1^b = -3.54$, if one uses for that purpose the representative values of nn and nnn coupling in the middle of the 11-layer slab ($J_{1\perp}^{S-4,S-5} = 1.66$ meV and $J_{2\perp}^{S-3,S-5} = -11.74$ meV). For an atom situated at the surface one has four nn plus four nnn couplings within the surface and four nn and one nnn coupling into the slab. Therefore, in this case the ratio is $(4J_{1\parallel}^{S} + 4J_{1\perp}^{S,S-1})/(4J_{2\parallel}^{S} + J_{2\perp}^{S,S-2}) = -3.53$ (using the coupling constants given in Sec. IV, $J_{1,2\perp}$ from the 11-layer slab calculation has been used) which is very similar to the bulk value. This could suggest why the surface Néel temperature of 529 K differs only very little from the bulk $T_N = 523.6$ K. However, for more rigorous conclusions one would need to do Monte Carlo simulations using the extracted trends of exchange coupling constants of this work.[49]

In conclusion, we have studied the electronic structure of bulk NiO and its (100) surface. We have shown that SIC-LSD improves the description of the electronic *and* magnetic structures, as compared to LSD. Along with predicting the experimentally found AF2 ordering as the ground state, the bulk exchange coupling constants show a better agreement with experiment. The SIC-LSD approach allows us to study

trends in the exchange coupling constants when moving from the bulk to the surface. The determined coupling constants at the (100) surface can be summarized as follows: the exchange coupling within the surface is slightly reduced, whereas the coupling perpendicular to the surface shows a pronounced enhancement, which is confined to coupling between the surface layer S, $(S-1)$, and $(S-2)$, respectively.

[1] V. Henrich and P. Cox, *The Surface Science of Metal Oxides* (Cambridge University Press, Cambridge, 1994).

[2] P. Cox, *Transition Metal Oxides: An Introduction to their Electronic Structure and Properties* (Clarendon Press, Oxford, 1992).

[3] J. Stöhr, A. Scholl, T.J. Regan, S. Anders, J. Lüning, M.R. Scheinfein, H.A. Padmore, and R.L. White, Phys. Rev. Lett. **83**, 1862 (1999).

[4] D. Alders, L.H. Tjeng, F.C. Voogt, T. Hibma, G.A. Sawatzky, C.T. Chen, J. Vogel, M. Sacchi, and S. Iacobucci, Phys. Rev. B **57**, 11 623 (1998).

[5] A. Barbier, C. Mocuta, H. Kuhlenbeck, K.F. Peters, B. Richter, and G. Renaud, Phys. Rev. Lett. **84**, 2897 (2000).

[6] F.Y. Yang and C.L. Chien, Phys. Rev. Lett. **85**, 2597 (2000).

[7] W. Zhu, L. Seve, R. Sears, B. Sinkovic, and S.S.P. Parkin, Phys. Rev. Lett. **86**, 5389 (2001).

[8] H. Ohldag, A. Scholl, F. Nolting, S. Anders, F.U. Hillebrecht, and J. Stöhr, Phys. Rev. Lett. **86**, 2878 (2001).

[9] G.A. Sawatzky and J.W. Allen, Phys. Rev. Lett. **53**, 2339 (1984).

[10] A. Svane and O. Gunnarsson, Phys. Rev. Lett. **65**, 1148 (1990).

[11] K. Terakura, T. Oguchi, A.R. Williams, and J. Kübler, Phys. Rev. B **30**, 4734 (1984).

[12] O.K. Andersen, H.L. Skriver, H. Nohl, and B. Johansson, Pure Appl. Chem. **52**, 93 (1979).

[13] V.I. Anisimov, F. Aryasetiawan, and A.I. Liechtenstein, J. Phys.: Condens. Matter **9**, 767 (1997).

[14] A.I. Liechtenstein and M.I. Katnelson, Phys. Rev. B **57**, 6884 (1998).

[15] Z. Szotek, W.M. Temmerman, and H. Winter, Phys. Rev. B **47**, 4029 (1993).

[16] F. Aryasetiawan and O. Gunnarsson, Phys. Rev. Lett. **74**, 3221 (1995).

[17] V. Anisimov, A. Poteryaev, M. Korotin, A. Anokhin, and G. Kotliar, J. Phys.: Condens. Matter **9**, 7359 (1997).

[18] M.D. Towler, N.L. Allan, N.M. Harrison, V.R. Saunders, W.C. Mackrodt, and E. Apra, Phys. Rev. B **50**, 5041 (1994).

[19] M. Marynowski, W. Franzen, M. El-Batanouny, and V. Staemmler, Phys. Rev. B **60**, 6053 (1999).

[20] C. de Graaf, F. Illas, R. Broer, and W. Nieuwpoort, J. Chem. Phys. **106**, 3287 (1997).

[21] J. Pothuizen, O. Cohen, and G. Sawatzky, in *Epitaxial Oxide Thin Films II*, edited by D.K. Fork, J.S. Speck, T. Shiosaki, and R.M. Wolf, MRS Symposia Proceedings No. 401 (Materials Research Society, Pittsburgh, PA, 1996), p. 501.

[22] M. Hutchings and E. Samuelsen, Phys. Rev. B **6**, 3447 (1972).

[23] G. Srinivasan and M.S. Seehra, Phys. Rev. B **29**, 6295 (1984).

[24] M.E. Lines, Phys. Rev. **139**, A1304 (1965).

[25] M.E. Lines, Phys. Rev. **139**, A1313 (1965).

[26] M.E. Lines, Phys. Rev. **135**, A1336 (1964).

[27] T. Lubensky and M. Rubin, Phys. Rev. B **12**, 3885 (1975).

[28] A. Bray and M. Moore, J. Phys. A **10**, 1927 (1977).

[29] A.I. Liechtenstein, M.I. Katnelson, V.P. Antropov, and V.A. Gubanov, J. Magn. Magn. Mater. **67**, 65 (1987).

[30] A. Liechtenstein, M. Katsnelson, and V. Gubanov, J. Phys. F **14**, L125 (1984).

[31] J.P. Perdew and A. Zunger, Phys. Rev. B **23**, 5048 (1981).

[32] Z. Szotek, W.M. Temmerman, and H. Winter, Solid State Commun. **74**, 1031 (1990).

[33] W.M. Temmerman, A. Svane, Z. Szotek, and H. Winter, in *Electronic Density Functional Theory: Recent Progress and New Directions*, edited by J.F. Dobson, G. Vignale, and P.M. Das (Plenum Press, New York, 1998).

[34] O.K. Andersen, Phys. Rev. B **12**, 3060 (1975).

[35] O.K. Andersen and O. Jepsen, Phys. Rev. Lett. **53**, 2571 (1984).

[36] W.R.L. Lambrecht and O.K. Andersen, Phys. Rev. B **34**, 2439 (1986).

[37] W.B. Pearson, *A Handbook of Lattice Spacings and Structures of Metals and Alloys* (Pergamon, New York, 1958).

[38] P. Dufek, P. Blaha, V. Sliwko, and K. Schwarz, Phys. Rev. B **49**, 10 170 (1994).

[39] H. Rooksby, Acta Crystallogr. **1**, 226 (1948).

[40] G. Slack, J. Appl. Phys. **31**, 1571 (1960).

[41] T. Oguchi, K. Terakura, and A.R. Williams, Phys. Rev. B **28**, 6443 (1983).

[42] M.R. Welton-Cook and M. Prutton, J. Phys. C **13**, 3993 (1980).

[43] C.G. Kinniburgh and J.A. Walker, Surf. Sci. **63**, 274 (1977).

[44] P. Palmberg, R. DeWames, and L. Vredevoe, Phys. Rev. Lett. **21**, 682 (1968).

[45] S.L. Dudarev, A.I. Liechtenstein, M.R. Castell, G.A.D. Briggs, and A.P. Sutton, Phys. Rev. B **56**, 4900 (1997).

[46] S. Sugano, Y. Tanabe, and H. Kamimura, *Multiplets of Transition-Metal Ions in Crystals* (Academic Press, New York, 1970).

[47] J. Zaanen, G.A. Sawatzky, and J.W. Allen, Phys. Rev. Lett. **55**, 418 (1985).

[48] C. de Graaf, R. Broer, and W. Nieuwport, Chem. Phys. Lett. **271**, 372 (1997).

[49] D.P. Landau and K. Binder, Phys. Rev. B **41**, 4633 (1990).